Journal of Medicinal Chemistry

Article

pubs.acs.org/jmc

Imaging Evaluation of $5HT_{2C}$ Agonists, [^{11}C]WAY-163909 and [^{11}C]Vabicaserin, Formed by Pictet–Spengler Cyclization

Ramesh Neelamegam,[†] Tim Hellenbrand,[‡] Frederick A. Schroeder,[†,§] Changning Wang,[†] and Jacob M. Hooker*[,†]

[†]Department of Radiology, Athinoula A. Martinos Center for Biomedical Imaging, Massachusetts General Hospital and Harvard Medical School, Charlestown, Massachusetts 02129, United States

[‡]Department of Pharmacy, Ludwig-Maximilians University, D-81377, Munich, Germany

[§]Center for Human Genetic Research, Department of Psychiatry, Massachusetts General Hospital and Harvard Medical School, Boston, Massachusetts 02114, United States

Supporting Information

ABSTRACT: The serotonin subtype 2C ($5HT_{2C}$) receptor is an emerging and promising drug target to treat several disorders of the human central nervous system. In this current report, two potent and selective $5HT_{2C}$ full agonists, WAY-163909 (**2**) and vabicaserin (**3**), were radiolabeled with carbon-11 via Pictet–Spengler cyclization with [^{11}C]formaldehyde and used in positron emission tomography (PET) imaging. Reaction conditions were optimized to exclude the major source of isotope dilution caused by the previously unknown breakdown of *N*,*N*-dimethylformamide (DMF) to formaldehyde at high temperature under mildly acid conditions. In vivo PET imaging was utilized to evaluate the pharmacokinetics and distribution of the carbon-11 labeled $5HT_{2C}$ agonists. Both radiolabeled molecules exhibit high blood–brain barrier (BBB) penetration and nonspecific binding, which was unaltered by preadministration of the unlabeled agonist. Our work demonstrates that Pictet–Spengler cyclization can be used to label drugs with carbon-11 to study their pharmacokinetics and for evaluation as PET radiotracers.

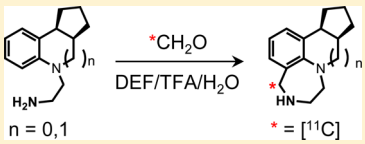

INTRODUCTION

The serotonin-2C receptor subtype ($5HT_{2C}$) is an important G-protein-coupled receptor that has been implicated in many central nervous system disorders including, among others, obesity, anxiety, and depression.[1−11] $5HT_{2C}$ receptors are distributed heterogeneously in the mammalian brain with high densities biased to subcortical regions such as the choroid plexus. Sufficient densities for imaging exist in the hypothalamus, globus pallidus, and substantia nigra. Lower densities of the receptors have been identified in the cortex and cerebellum.[12−14] Of the diseases $5HT_{2C}$ has been shown to cause or contribute to, obesity has been at the forefront of research, and new drugs targeting $5HT_{2C}$ (e.g., lorcaserin, hereafter referred as **1**) are the first gaining Food and Drug Administration (FDA) approval in more than a decade.[15,16] To date, a number of $5HT_{2C}$ agonists (Figure 1) have been generated and used in preclinical and clinical studies.[8,17] In addition to a functional role in eating disorders, the receptor has also been implicated in mood behavior, for example, by mediating effects of selective serotonin reuptake inhibitors (SSRIs) and atypical antipsychotics.[18−20]

Although many studies suggest that dysfunction of $5HT_{2C}$ receptors contribute to important brain-related disorders,[1−11] direct links between these diseases and $5HT_{2C}$ receptor abnormalities have been difficult to elucidate. This is in part due to the lack of a method for determining $5HT_{2C}$ receptor concentration as a function of disease in humans. We have previously labeled and evaluated arylazepines[21] as ligands for positron emission tomography; however, direct carbon-11 incorporation into some of the most promising lead candidates (certain benzodiazepines) was difficult because no pendent methyl group or fluorine was available for PET isotope substitution. Two molecules of particular interest as scaffolds for ligand development were thus inaccessible because of limitations in reaction methods for carbon-11 incorporation. The potent and selective compounds **2** (WAY-163909) and **3** (vabicaserin) are agonists that exhibit high affinity (K_i of ∼10 and 3 nM, respectively) and good efficacy for $5HT_{2C}$ (EC_{50} = 8 nM each) and have been characterized extensively in preclinical drug trials.[8,9,22−24]

In order to overcome the synthesis challenge of carbon-11 incorporation for **2** and **3**, [^{11}C]formaldehyde was used in a Pictet–Spengler cyclization. Using an in situ formation method of [^{11}C]formaldehyde from [^{11}C]methyl iodide developed in our lab,[25] we were able to prepare [^{11}C]**2** and [^{11}C]**3** . In the process of doing so, we determined that under the acidic conditions required for product formation, the solvent DMF degrades to generate formaldehyde, consequently reducing the specific radioactivity of the product. Through detailed isotope utilization (deuterium and carbon-13) we pinpointed and eliminated the sources of formaldehyde while simultaneously demonstrating that in situ formation of isotopically labeled formaldehyde is generalizable and can be used to install carbon

Received: November 21, 2013
Published: February 3, 2014

   dx.doi.org/10.1021/jm401802f | *J. Med. Chem.* 2014, 57, 1488−1494

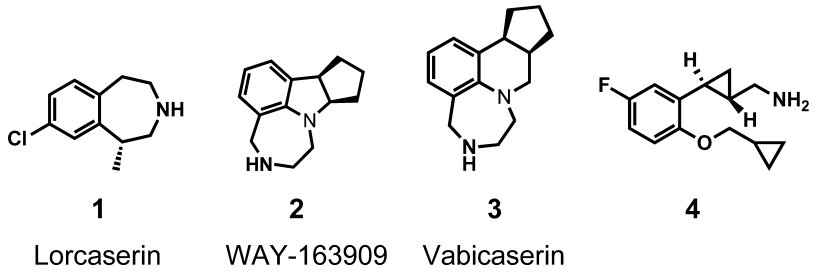

Figure 1. $5HT_{2C}$ receptor full agonists in preclinical and clinical studies.

Scheme 1. Synthesis of WAY-163909 Labeling Precursor (11) and Reference Standard (2)[a]

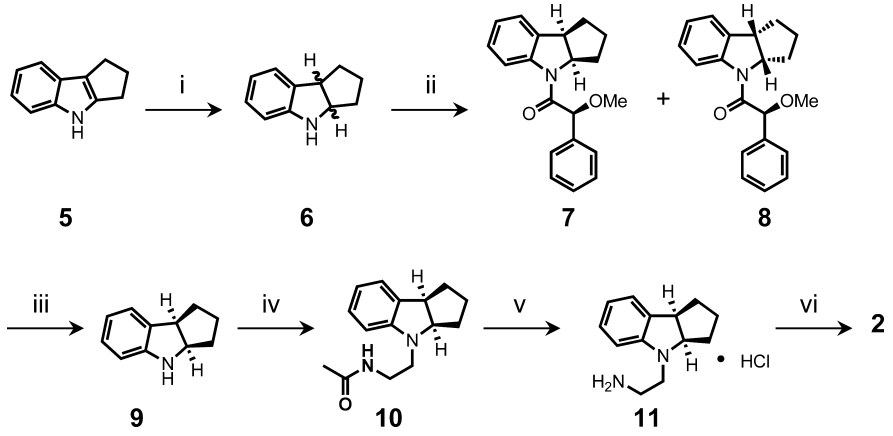

[a]Reagents and conditions: (i) H_2 (45 psi), 5% Pd/C, EtOH, rt, 65%; (ii) (a) (*S*)-2-methoxy-2-phenylacetyl chloride, Et_3N, DCM; (b) separation by column chromatography, 30%; (iii) dilute H_2SO_4, 70 °C, 8 h, 30%; (iv) 2-methyl-2-oxazoline, *p*TsOH (cat.), 165 °C, 3 h, 50%; (v) (a) dilute H_2SO_4, 70 °C, 8 h; (b) aq NaOH; (c) 2.0 M Et_2O–HCl, rt, 50% (three steps), 97% ee; (vi) 37% aq HCHO, TFA/EtOH, rt, 70%.

Scheme 2. Synthesis of Vabicaserin Labeling Precursor (18) and Reference Standard (3)[a]

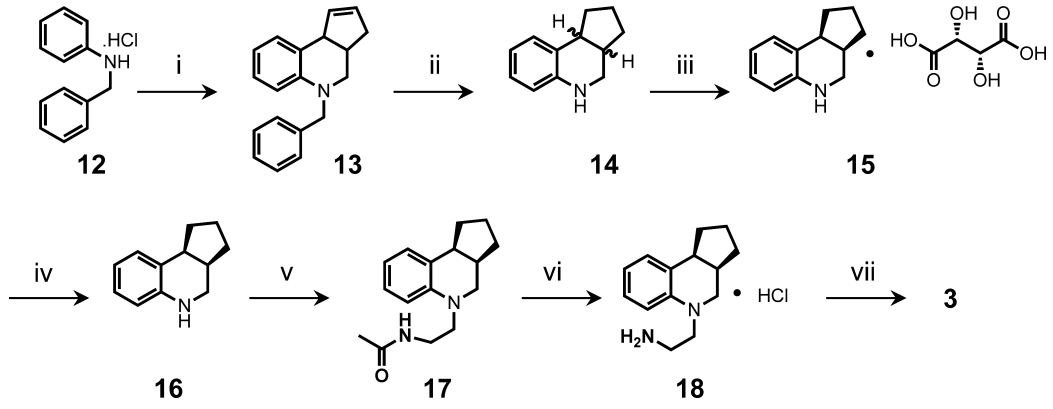

[a]Reagents and conditions: (i) cyclopentadiene, 37% aq HCHO/HCl, EtOH, 5 °C, 10 h; (ii) H_2 (45 psi)/10% Pd/C, EtOH/EtOAc (1:1), rt, 10 h, 65%; (iii) (a) ditoluoyl-D-tartaric acid, IPA; (b) separation by crystallization, 30%; (iv) 5% aq NaOH, 90%, 97.5% ee; (v) 2-methyl-2-oxazoline, *p*TsOH (cat.), 165 °C, 3 h, 55%; (vi) (a) dilute H_2SO_4, 70 °C, 8 h; (b) aq NaOH; (c) 2.0 M Et_2O–HCl, rt, 50% (three steps), 97% ee; (vii) 37% aq HCHO, TFA/EtOH, rt, 60%.

and hydrogen isotopes (singly or in concert). These isotopalogs may themselves warrant preclinical drug evaluation. We further demonstrate that high specific activity [^{11}C]**2** and [^{11}C]**3**, and by extension derivatives thereof, can be synthesized. Finally, we evaluated the potential of [^{11}C]**2** and [^{11}C]**3** as scaffolds for PET radiotracer development. Both molecules exhibit high brain uptake in rats and non-human primates dominated by nonspecific binding which we are now in the process of tuning through structure modification.

RESULTS AND DISCUSSION

Chemistry. Retrosynthetic analyses of **2** and **3** were possible provided that carbon-11 could be incorporated at the last step of the synthesis and provided that the corresponding primary amines (precursors **11** and **18**) could be derived. Schemes 1 and 2 represent our routes to syntheses of precursors **11** and **18**, respectively. The development of a synthesis route for preparing chiral labeling precursors **11** and **18** were more challenging than expected. For **2** synthesis, neither chiral crystallization of **6** with (−)-2,3-dibenzoyl-L-tartaric acid and

dx.doi.org/10.1021/jm401802f | *J. Med. Chem.* 2014, 57, 1488–1494

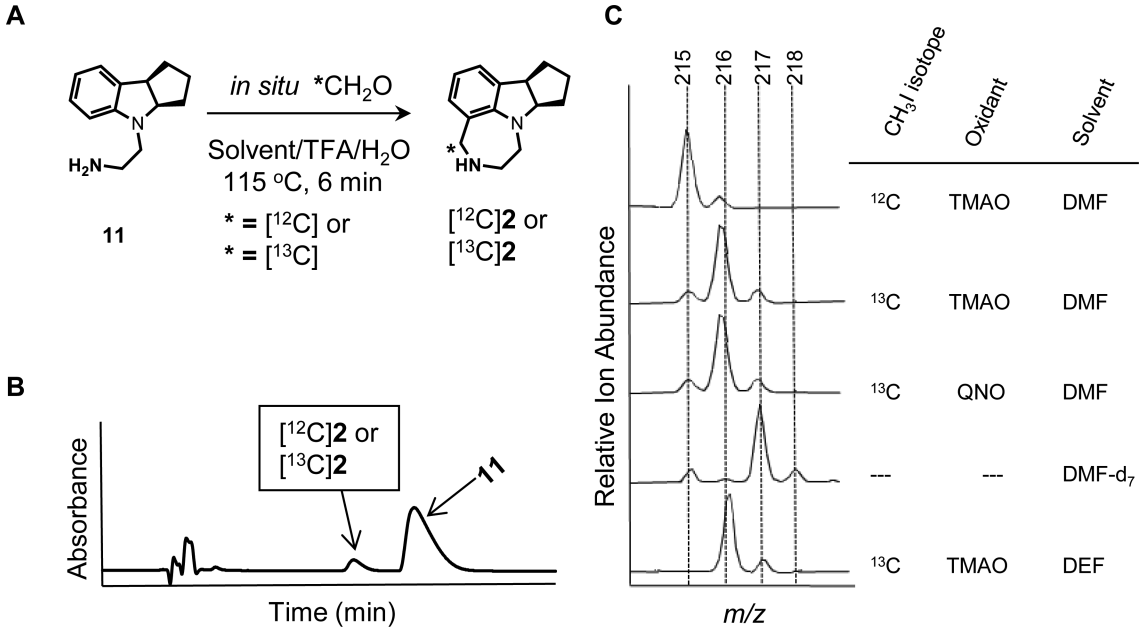

Figure 2. Experiments to determine mechanism of specific activity erosion. (A) Synthesis of [*C]**2** using in situ generated [*C]CH_2O (generated from [*C]CH_3I/oxidant/solvent at 80 °C for 3 min). (B) Aliquots of the reaction mixture injected in the LC−MS instrument (UV, 254 nm). (C) Taken together, these data shown [^{12}C]CH_2O are generated from DMF and TFA at elevated temperatures. DMF should be avoided for high specific activity.

ditoluyl-D-tartartic acid nor resolution of diastereomers following reaction of **6** with 1*S*-(+)-10-camphorsulfonyl chloride was successful. Reaction of racemic **6** with a chiral mandelic acid derivative [(*R*)-(−)-*α*-methoxyphenylacetic acid] was ultimately successful. To isolate optically active materials, racemic compound **6** was treated with an enantiopure (*R*)-(−)-*α*-methoxyphenylacetyl chloride to give two diastereomers **7** and **8**. Separation of diastereomer **7** was achieved by column chromatography, and the structures of **7** and **8** were confirmed by single crystal X-ray diffraction (XRD) analysis (Figure 1 in Supporting Information). Removal of the mandelic acid derived chiral auxiliary cleavage to afford enantio-enriched **11** was not initially achieved using conditions predicted from the literature to proceed efficiently (these attempts included 1.0 M LAH in THF, saturated HCl in methanol at reflux, 5% NaOH in methanol at reflux, and lithium triethylborohydride (super-hydride)). Fortunately, the use of dilute sulfuric acid at moderate temperatures (65 °C) did provide **7** albeit in moderate yield. More harsh conditions led to decomposition to unidentified products. Nonetheless, sufficient (multimilligram) quantities of the chiral precursor to **2** (enantiomeric excess of 97%) were obtained for carbon-11 labeling (Scheme 1).

The synthesis of **3** and its precursor **18** followed the published patent procedures.[26] Resolution of the precursor enantiomers was achieved by cocrystallization of an early intermediate using ditoluyl-D-tartartic acid (Scheme 2). Using this route, we were able to produce **18** for use in carbon-11 radiochemistry and PET imaging. Reference compounds **2** and **3** were synthesized from precursors **11** and **18**, respectively, using a Pictet−Spengler cyclization with formaldehyde under conditions optimal for isolated yield but not for radiochemical synthesis.

To optimize labeling conditions for carbon-11, we needed to dramatically reduce the reaction time required for formaldehyde condensation and cyclization due to the short carbon half-life ($t_{1/2}$ = 20.4 min). Moreover, we needed to adapt the cyclization method to be compatible (in a one-pot strategy) with conditions for in situ generation of [^{11}C]formaldehyde from [^{11}C]methyl iodide. Initially we determined that **2** could be formed from **11** at a high temperature (115 °C) in DMF and trifluoroacetic acid (TFA) using nonradioactive in situ [^{12}C]CH_2O (generated from substoichiometric amounts of [^{12}C]CH_3I with an oxidant, trimethylamine *N*-oxide (TMAO)). Reactions with *N*-methylmorpholine-*N*-oxide (NMMNO) and quinuclidine *N*-oxide (QNO) were successful but provided lower yield than TMAO. TMAO is also commercially available and inexpensive.[25] To further confirm the labeling position and compound identity, we used substoichiometric [^{13}C]CH_3I and an excess of TMAO in DMF at 80 °C followed by treatment with precursor **11**, TFA, and H_2O at 115 °C to enrich the expected 50 ppm resonance observed by ^{13}C NMR. Analysis of the [^{13}C]**2** by LC−-MS lead to the observation of an isotope distribution suggestive of isotopic dilution (i.e., the 99% enriched [^{13}C]CH_3I led to a product on 80−90% enriched). Dilution of the isotope when applied in the context of carbon-11 was indeed determined to provide isolated products with unacceptably low specific radioactivity (0.02 mCi/nmol) for proper evaluation as a PET radiotracer for $5HT_{2C}$ receptors.

To determine the source of [^{12}C]CH_2O, we systematically replaced each reaction component starting with the two methyl sources TMAO and DMF. Previously, we had determined that TMAO under milder conditions did not decompose to form formaldehyde, but in order to completely rule out the contribution from TMAO, we synthesized an oxidant without methyl groups, QNO. Under the same reaction conditions used with TMAO and in the presence of only [^{13}C]CH_3I, we observed the formation of [^{12}C]**2** by LC−MS (Figure 2C). By use of perdeuterated *N*,*N*-dimethylformamide (DMF-d_7) as solvent, deuterium incorporation was observed by LC−MS (product *m*/*z*, 217; Figure 2 in Supporting Information), indicating that decomposition of DMF-d_7 to formaldehyde-d_2

dx.doi.org/10.1021/jm401802f | J. Med. Chem. 2014, 57, 1488−1494

(CD_2O) occurs at high temperatures under mild acidic conditions. We are unaware of existing data in the literature describing the formation of formaldehyde from DMF and have not yet made steps toward elucidating a potential reaction mechanism, although these steps are planned.

For the present goal unintended formaldehyde formation was prevented by replacing DMF with *N*,*N*-diethylformamide (DEF). Presumably, DEF can decompose (by analogue) to acetaldehyde, but we did not observe reaction products by LC–MS indicative of the subsequent condensation and cyclization of **11** with acetaldehyde. Satisfyingly, under reaction conditions with DEF no isotopic dilution was observed using $[^{13}C]CH_3I$ with either TMAO or QNO as the oxidant to generate $[^{13}C]CH_2O$. Ultimately, TMAO in DEF with TFA proved to be the most efficient conditions for carbon-11 labeling, and under these conditions we were able to isolate high specific radioactivity products.

Radiolabeling of [^{11}C]2 and [^{11}C]3. After optimization, with a good chemical synthesis method in hand to prevent isotope dilution while affecting the reaction in reasonable reaction times, carbon-11 radiolabeling procedures was performed as follows for imaging: an amount of 4 mg of TMAO was dissolved in DEF and cooled to −10 °C in a reactor, and $[^{11}C]CH_3I$ was trapped. Then the mixture was heated to 80 °C for 3 min. In a separate vial 1.2 ± 0.3 mg of the alkylamines, **11**/**18**, was dissolved in a mixture of DEF, water, and TFA. This solution was then transferred into the reaction vial, and heating was continued at 115 °C for 6 min (Scheme 3). To quench the reaction, 1 mL of 0.1% formic acid was added, and the entire reaction mixture was purified by reversed-phase semipreparative HPLC. The final product was reformulated into 10% EtOH with saline using C-18 solid-phase exchange (SPE). The chemical and radiochemical purity of the final products, [^{11}C]**2** and [^{11}C]**3**, were tested by analytical HPLC. The identities of the respective products were confirmed by analytical HPLC with additional co-injection of corresponding reference standards (Figures 3 and 4 in Supporting Information). The average time required for the synthesis from end of cyclotron bombardment to end of synthesis and purification was 50 min [^{11}C]**2** and [^{11}C]**3**. The average radiochemical yield was [^{11}C]**2** (1.5 ± 0.5%; decay-corrected to trapped $[^{11}C]CH_3I$; n = 3) and [^{11}C]**3** (1.3 ± 0.2%; decay-corrected to trapped $[^{11}C]CH_3I$; n = 3). Chemical and radiochemical purities were >97% in all instances. Specific activities of [^{11}C]**2** and [^{11}C]**3** were 0.85 ± 0.2 mCi/nmol (n = 3) and 1.18 ± 0.20 mCi/nmol (n = 3), respectively, at the end of synthesis (EOS).

Scheme 3. Radiosynthesis of [^{11}C]2 and [^{11}C]3 Using in Situ $[^{11}C]CH_2O$ (Generated from $[^{11}C]CH_3I/Me_3N^+O^-$/DEF at 80 °C for 3 min)[a]

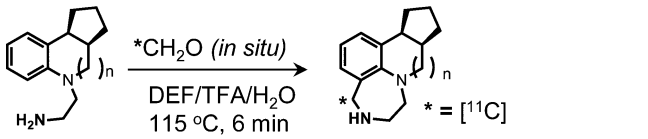

n=0 **(11)**
n=1 **(18)**

n=0 **[^{11}C]2** (RCY = 1.5 ± 0.5%)
n=1 **[^{11}C]3** (RCY = 1.3 ± 0.2%)

[a]RCY is an isolated, formulated, and decay corrected yield.

Preliminary Imaging Evaluation of [^{11}C]2 and [^{11}C]3. Using a small animal PET-CT, we determined that both [^{11}C]**2** and [^{11}C]**3** exhibited high initial blood–brain barrier (BBB) penetration and good retention in the brain over the scanning time (60 min) when administered intravenously to Sprague–Dawley rats (Figure 3). Although whole-brain time–activity curves generated from imaging data are presented, heterogeneous binding was observed for both labeled compounds. In order to determine the sensitivity of uptake to pretreatment (and potential saturation of the $5HT_{2C}$ receptor sites), rodents were pretreated in separate experiments with the corresponding unlabeled ligand (e.g., **3**, 1 mg/kg iv, was administered 5 min prior to [^{11}C]**3** imaging). Pharmacokinetics of [^{11}C]**2** were altered by drug treatment; pharmacokinetics of [^{11}C]**3** were not. The more rapid washout of [^{11}C]**2** can be attributed to several phenomena including receptor saturation, changes in arterial plasma concentration, or changes in metabolism. We were encouraged by the data to further evaluate specificity (saturability) of [^{11}C]**2** binding and thus moved to non-human primates where we have extensive experience performing MR-PET imaging with arterial-derived and metabolite corrected blood data.[21,27]

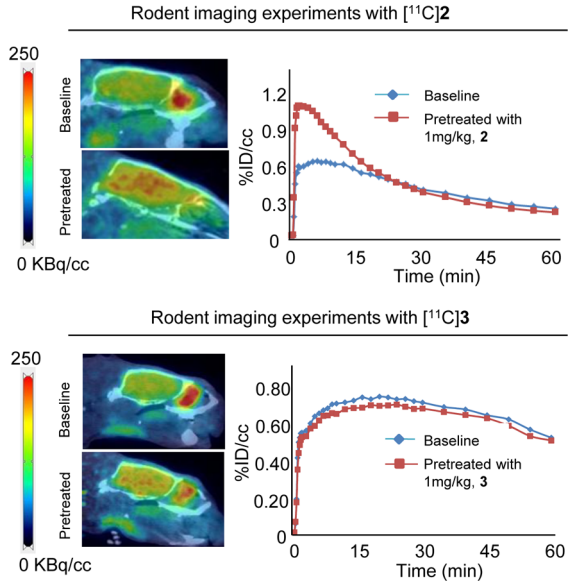

Figure 3. Top: Summed PET images (0–60 min) following injection of [^{11}C]**2**: baseline scan (0.265 mCi); image acquired following pretreatment (5 min prior) with **2** (1 mg/kg, 0.303 mCi). Images are dose corrected. Bottom: Summed PET images (0–60 min) following injection of [^{11}C]**3**: baseline scan (0.96 mCi); image acquired following pretreatment (5 min prior) with **3** (1 mg/kg, 0.99 mCi). Images are dose corrected. Whole-brain time–activity curves were generated from imaging data.

Evaluation of [^{11}C]2 in *Papio anubis* Baboon. Prior to non-human primate imaging, we experimentally determined that the partition coefficient (log D) between pH 7.4 phosphate buffered saline (PBS) and octanol was 1.53 ± 0.13 (n = 3). In addition, the predisposition of [^{11}C]**2** to bind plasma protein (ppb) was determined with a baboon plasma sample after 10 min of incubation time at room temperature. Relatively high (26.5 ± 0.30%) amounts of [^{11}C]**2** were free at equilibrium which was encouraging given previously reported correlations between plasma protein binding and nonspecific brain homogenate binding.[28,29]

To further investigate the brain permeability of [^{11}C]**2** and specific binding to $5HT_{2C}$ receptors, we administered the

dx.doi.org/10.1021/jm401802f | J. Med. Chem. 2014, 57, 1488–1494

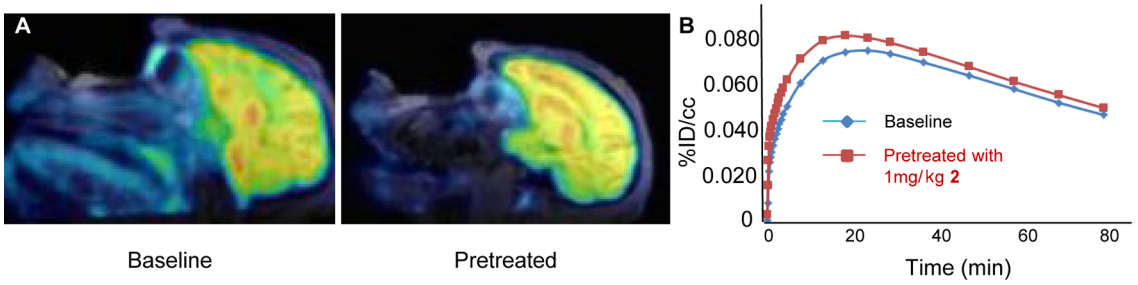

Figure 4. (A) Summed PET images (0–80 min) following injection of [^{11}C]**2**: (left) baseline scan (2.08 mCi); (middle) image acquired following pretreatment (10 min prior) with **2** (1 mg/kg, 2.33 mCi). Images are dose corrected. (B) Whole-brain time–activity curves generated from PET imaging data. Maximum uptake is observed at 20 min after injection. Neither a reduction in uptake nor a change in the distribution or kinetics was observed between the baseline and blocking curves.

labeled compound in a paired baseline/pretreatment protocol to *Papio anubis* baboon. As in rodents, [^{11}C]**2** exhibited very good BBB penetration and high brain uptake over the scanning time (80 min) when the [^{11}C]**2** (2.08 mCi) was administered intravenously (Figure 4A). Unlike in rodents, pretreatment with **2** (1 mg/kg, 2.33 mCi) 10 min prior to injection of [^{11}C]**2** did not alter the pharmacokinetics of radioactivity in the whole brain. Time–activity curves generated from PET imaging data provided that maximal uptake occurs at 20 min after injection. Neither a reduction in uptake nor a change in the distribution or kinetics was observed between the baseline and blocking dose curves (Figure 4B). Arterial blood samples indicated that there was no change in blood half-life or in compound metabolism. The differences in TACs for rodents and NHPs (as well as other species) are not fully understood but also not uncommonly observed. Current understanding of the expression of 5HT$_{2C}$ receptors in rat and non-human primate brain indicates an overall similarity, with differences noted in subregions including the neocortex, hippocampal subfields, and substantia nigra,[30,31] and range in density from ∼50 to 150 fmol/mg protein.[32,33] Little is described about 5HT$_{2C}$ receptors outside the brain. We noticed in rat a robust uptake of [^{11}C]**2** in regions outside the brain but within the skull (Figure 3 top, baseline, blue). This accumulation may comprise olfactory epithelium or lacrimal glands, two components modulated by serotonin. Pretreatment with unlabeled **2** decreased binding in these peripheral target sites, resulting in altered pharmacokinetics of the tracer. This was evidenced by a vertical shift in early time points of the time–activity curve, to a large extent in rat (Figure 3 top) and less so in baboon (Figure 4). Further studies are warranted to quantify species differences in non-CNS 5HT$_{2C}$ receptors and understand their role in 5-HT signaling within the brain. Combined, these data suggest that the signal from [^{11}C]**2** and/or its metabolites in the non-human primate brain is nonspecific and not an indicator of 5HT$_{2C}$ distribution and density. Nonetheless, given the favorable properties of low PPB, good metabolic stability, appropriate lipophilicity, and high BBB penetration, **2** is a good scaffold for further derivation.

CONCLUSIONS

We have developed a one-pot, two-step synthesis of [^{11}C]**2** and [^{11}C]**3** by using a Pictet–Spengler type cyclization with in situ generated high specific activity [^{11}C]formaldehyde. We isolated sources of isotopic dilution and have provided a general set of reaction conditions for labeling certain benzodiazepines isotopically (both stable and unstable) at benzylic position. We accomplished the first PET imaging evaluation of two important 5HT$_{2C}$ receptor agonists in both rat and baboon and have provided insight into CNS pharmacokinetics. Both [^{11}C]**2** and [^{11}C]**3** exhibit rapid and high brain uptake but with high nonspecific binding (not necessarily a negative feature for use of these compounds as preclinical pharmacology tools). Our radiolabeling strategy is adaptable, and future work will be well positioned to radiolabel additional 5HT$_{2C}$ drugs or any tracers to investigate the serotonergic system and others in using PET imaging.

ASSOCIATED CONTENT

Supporting Information

Synthetic procedures, characterization data, radiochemistry, and acquisition details for in vivo imaging studies. This material is available free of charge via the Internet at http://pubs.acs.org.

AUTHOR INFORMATION

Corresponding Author

*Telephone: 617-726-6596. Fax: 617-726-7422. E-mail: hooker@nmr.mgh.harvard.edu. Address: Athinoula A. Martinos Center for Biomedical Imaging, Building 149, 13th Street, Suite 2301, Charlestown, MA 02129.

Notes

The authors declare no competing financial interest.

ACKNOWLEDGMENTS

This research was carried out at the Athinoula A. Martinos Center for Biomedical Imaging at the Massachusetts General Hospital, using resources provided by the Center for Functional Neuroimaging Technologies, P41EB015896, a P41 Regional Resource supported by the National Institute of Biomedical Imaging and Bioengineering (NIBIB), National Institutes of Health. This project was funded by a grant from the National Institutes of Health (Grant 1R21MH093874). This work also involved the use of instrumentation supported by the NIH Shared Instrumentation Grant Program and/or High-End Instrumentation Grant Program, specifically, Grants S10RR017208, S10RR026666, S10RR022976, S10RR019933, and S10RR029495. We thank members of the Hooker research laboratory for helpful discussions. The authors are grateful to Grae Arabasz, Shirley Hsu, Joseph Mandeville, and Helen Deng for assistance during NHP imaging and to Christian Moseley and Stephen Carlin for technical assistance in the radiochemistry laboratory. The authors also thank Prof. Ritter's research group, Department of Chemistry, Harvard University, MA, for single crystal X-ray data collection.

■ ABBREVIATIONS USED

PET-CT, positron emission tomography−computated tomography; DMF, *N*,*N*-dimethylformamide; DMSO, dimethyl sulfoxide; DEF, *N*,*N*-diethylformamide; THF, tetrahydrofuran; DMF-d_7, *N*,*N*-dimethylformamide-d_7; LAH, lithium aluminum hydride; TMAO, trimethylamine *N*-oxide; QNO, quinuclidine *N*-oxide; TFA, trifluoroacetic acid; PBS, phosphate buffered saline; FDA, Food and Drug Administration; NHP, non-human primate; TAC, time−activity curve; BBB, blood−brain barrier; PPB, plasma protein binding; XRD, X-ray diffraction

■ REFERENCES

(1) Tecott, L. H.; Sun, L. M.; Akana, S. F.; Strack, A. M.; Lowenstein, D. H.; Dallman, M. F.; Julius, D. Eating disorder and epilepsy in mice lacking 5-HT2c serotonin receptors. *Nature* **1995**, *374*, 542−546.

(2) Nonogaki, K.; Strack, A. M.; Dallman, M. F.; Tecott, L. H. Leptin-independent hyperphagia and type 2 diabetes in mice with a mutated serotonin 5-HT2C receptor gene. *Nat. Med.* **1998**, *4*, 1152−1156.

(3) Somerville, E. M.; Horwood, J. M.; Lee, M. D.; Kennett, G. A.; Clifton, P. G. 5-HT2C receptor activation inhibits appetitive and consummatory components of feeding and increases brain c-fos immunoreactivity in mice. *Eur. J. Neurosci.* **2007**, *25*, 3115−3124.

(4) Rosenzweig-Lipson, S. Therapeutic combinations for the treatment of depression. U.S. Patent US 2007/0225279 A1, 2007.

(5) Christianson, J. P.; Ragole, T.; Amat, J.; Greenwood, B. N.; Strong, P. V.; Paul, E. D.; Fleshner, M.; Watkins, L. R.; Maier, S. F. 5-Hydroxytryptamine 2C receptors in the basolateral amygdala are involved in the expression of anxiety after uncontrollable traumatic stress. *Biol. Psychiatry* **2010**, *67*, 339−345.

(6) von Meyenburg, C.; Langhans, W.; Hrupka, B. J. Evidence that the anorexia induced by lipopolysaccharide is mediated by the 5-HT2C receptor. *Pharmacol., Biochem. Behav.* **2003**, *74*, 505−512.

(7) Rowland, N. E.; Crump, E. M.; Nguyen, N.; Robertson, K.; Sun, Z.; Booth, R. G. Effect of (−)-*trans*-PAT, a novel 5-HT2C receptor agonist, on intake of palatable food in mice. *Pharmacol., Biochem. Behav.* **2008**, *91*, 176−180.

(8) Dunlop, J.; Marquis, K. L.; Lim, H.; Leung, L.; Kao, J.; Cheesman, C.; Rosenzweig-Lipson, S. Pharmacological profile of the 5-HT2C receptor agonist WAY-163909; therapeutic potential in multiple indications. *CNS Drug Rev.* **2006**, *12*, 167−177.

(9) Dunlop, J.; Sabb, A. L.; Mazandarani, H.; Zhang, J.; Kalgaonker, S.; Shukhina, E.; Sukoff, S.; Vogel, R. L.; Stack, G.; Schechter, L. WAY-163909 [(7bR,10aR)-1,2,3,4,8,9,10,10a-octahydro-7bH-cyclopenta-[b][1,4]diazepino[6,7,1hi]indole], a novel 5-hydroxytryptamine 2C receptor-selective agonist with anorectic activity. *J. Pharmacol. Exp. Ther.* **2005**, *313*, 862−869.

(10) Kroeze, W.; Roth, B. The molecular biology of serotonin receptors: therapeutic implications for the interface of mood and psychosis. *Biol. Psychiatry* **1998**, *44*, 1128−1142.

(11) Baldwin, D.; Rudge, S. The role of serotonin in depression and anxiety. *Int. Clin. Psychopharmacol.* **1995**, *9* (Suppl. 4), 41−45.

(12) Pompeiano, M.; Palacios, J.; Mengod, G. Distribution of the serotonin 5-HT2 receptor family mRNAs: comparison between 5-HT2A and 5-HT2C receptors. *Mol. Brain Res.* **1994**, *23*, 163−178.

(13) Abramowski, D.; Rigo, M.; Duc, D.; Hoyer, D.; Staufenbiel, M. Localization of the 5-hydroxytryptamine 2C receptor protein in human and rat brain using specific antisera. *Neuropharmacology* **1995**, *34*, 1635−1645.

(14) Eberle-Wang, K.; Mikeladze, Z.; Uryu, K.; Chesselet, M. F. Pattern of expression of the serotonin2C receptor messenger RNA in the basal ganglia of adult rats. *J. Comp. Neurol.* **1997**, *384*, 233−247.

(15) Thomsen, W. J.; Grottick, A. J.; Menzaghi, F.; Reyes-Saldana, H.; Espitia, S.; Yuskin, D.; Whelan, K.; Martin, M.; Morgan, M.; Chen, W. Lorcaserin, a novel selective human 5-hydroxytryptamine2C agonist: in vitro and in vivo pharmacological characterization. *J. Pharmacol. Exp. Ther.* **2008**, *325*, 577−587.

(16) Pauli, M.; Abdelghany, S. Lorcaserin: a novel, selective 5-HT2C-receptor agonist for the treatment of obesity. *Formulary* **2010**, *45*, 180−186.

(17) Chen, G.; Cho, S. J.; Huang, X.-P.; Jensen, N. H.; Svennebring, A.; Sassano, M. F.; Roth, B. L.; Kozikowski, A. P. Rational drug design leading to the identification of a potent 5-HT_{2C} agonist lacking 5-HT_{2B} activity. *ACS Med. Chem. Lett.* **2011**, *2*, 929−932.

(18) Millan, M. J.; Gobert, A.; Lejeune, F.; Dekeyne, A.; Newman-Tancredi, A.; Pasteau, V.; Rivet, J.-M.; Cussac, D. The novel melatonin agonist agomelatine (S20098) is an antagonist at 5-hydroxytryptamine2C receptors, blockade of which enhances the activity of frontocortical dopaminergic and adrenergic pathways. *J. Pharmacol. Exp. Ther.* **2003**, *306*, 954−964.

(19) Millan, M.; Girardon, S.; Dekeyne, A. 5-HT2C receptors are involved in the discriminative stimulus effects of citalopram in rats. *Psychopharmacology* **1999**, *142*, 432−434.

(20) Hackler, E. A.; Turner, G. H.; Gresch, P. J.; Sengupta, S.; Deutch, A. Y.; Avison, M. J.; Gore, J. C.; Sanders-Bush, E. 5-Hydroxytryptamine2C receptor contribution to *m*-chlorophenylpiperazine and *N*-methyl-*β*-carboline-3-carboxamide-induced anxiety-like behavior and limbic brain activation. *J. Pharmacol. Exp. Ther.* **2007**, *320*, 1023−1029.

(21) Granda, M. L.; Carlin, S. M.; Moseley, C. K.; Neelamegam, R.; Mandeville, J. B.; Hooker, J. M. Synthesis and evaluation of methylated arylazepine compounds for PET imaging of 5-HT2c receptors. *ACS Chem. Neurosci.* **2013**, *4*, 261−265.

(22) Grauer, S. M.; Graf, R.; Navarra, R.; Sung, A.; Logue, S. F.; Stack, G.; Huselton, C.; Liu, Z.; Comery, T. A.; Marquis, K. L. WAY-163909, a 5-HT2C agonist, enhances the preclinical potency of current antipsychotics. *Psychopharmacology* **2009**, *204*, 37−48.

(23) Navarra, R.; Comery, T. A.; Graf, R.; Rosenzweig-Lipson, S.; Day, M. The 5-HT2C receptor agonist WAY-163909 decreases impulsivity in the 5-choice serial reaction time test. *Behav. Brain Res.* **2008**, *188*, 412−415.

(24) Marquis, K. L.; Sabb, A. L.; Logue, S. F.; Brennan, J. A.; Piesla, M. J.; Comery, T. A.; Grauer, S. M.; Ashby, C. R.; Nguyen, H. Q.; Dawson, L. A. WAY-163909 [(7bR,10aR)-1,2,3,4,8,9,10,10a-octahydro-7bH-cyclopenta-[b][1,4]diazepino[6,7,1hi]indole]: a novel 5-hydroxytryptamine 2C receptor-selective agonist with preclinical antipsychotic-like activity. *J. Pharmacol. Exp. Ther.* **2007**, *320*, 486−496.

(25) Hooker, J. M.; Schönberger, M.; Schieferstein, H.; Fowler, J. S. A simple, rapid method for the preparation of [^{11}C] formaldehyde. *Angew. Chem., Int. Ed.* **2008**, *47*, 5989−5992.

(26) Megati, S.; Bhansali, S.; Dehnhardt, C.; Deshmukh, S.; Fung, P.; Macewan, M.; Tinder, R. J. Chiral synthesis of diazepinoquinolines. EP Patent 2,203,450, 2010.

(27) Wang, C.; Wilson, C. M.; Moseley, C. K.; Carlin, S. M.; Hsu, S.; Arabasz, G.; Schroeder, F. A.; Sander, C. Y.; Hooker, J. M. Evaluation of potential PET imaging probes for the orexin 2 receptors. *Nucl. Med. Biol.* **2013**, *40*, 1000−1005.

(28) Laruelle, M.; Slifstein, M.; Huang, Y. Relationships between radiotracer properties and image quality in molecular imaging of the brain with positron emission tomography. *Mol. Imaging Biol.* **2003**, *5*, 363−375.

(29) Trainor, G. L. The importance of plasma protein binding in drug discovery. *Expert Opin. Drug Discovery* **2007**, *2*, 51−64.

(30) Mengod, G. Serotonin 5-HT2C Receptors: Chemical Neuronatomy in the Mammalian Brain. In *5-HT2C Receptors in the Pathophysiology of CNS Disease*; Di Giovanni, G., Esposito, E., Di Matteo, V., Eds.; Springer: New York, 2011; pp 17−27.

(31) Mengod, G.; Pompeiano, M.; Palacios, J. Localization of the mRNA for the 5-HT2 receptor by in situ hybridization histochemistry. Correlation with the distribution of receptor sites. *Brain Res.* **1990**, *524*, 139−143.

(32) Pandey, S. C.; Dubey, M. P.; Piano, M. R.; Schwertz, D. W.; Davis, J. M.; Pandey, G. N. Modulation of 5-HT1C receptors and phosphoinositide system by ethanol consumption in rat brain and choroid plexus. *Eur. J. Pharmacol.* **1993**, *247*, 81−88.

(33) Wolf, W. A.; Schutz, L. J. The serotonin 5-HT2C receptor is a prominent serotonin receptor in basal ganglia: evidence from functional studies on serotonin-mediated phosphoinositide hydrolysis. *J. Neurochem.* **1997**, *69*, 1449−1458.